

Supporting Information

High-Efficiency Synthesis of Enhanced-Titanium and Anatase-Free TS-1 Zeolite by Using Crystallization Modifier

Jiani Zhang, ‡ Huaizhong Shi, ‡ Yue Song, Wenjing Xu, Xianyu Meng, Jiyang Li*

State Key Laboratory of Inorganic Synthesis & Preparative Chemistry, College of Chemistry, Jilin University, Changchun 130012, P. R. China.

* Corresponding author. E-mail address: lijiyang@jlu.edu.cn

‡ Equally contributed to this work.

Fig. S1 N ₂ adsorption–desorption isotherms of NTS-61H and NTS-73H.	2
Fig. S2 The XPS spectra of Ti 2p of samples.	2
Fig. S3 ²⁹ Si MAS NMR spectra of NTS-61H and CTS-1.	3
Fig. S4 Photos of initial synthetic mixtures.	3
Fig. S5 XRD patterns of NTS-0H-xh and NTS-61H-xh.	4
Fig. S6 TEM images of NTS-61H-xh.	4
Fig. S7 TEM images of NTS-0H-xh.	5
Fig. S8 Respective yields of Ti in NTS-0H-xh and NTS-61H-xh.	5
Fig. S9 UV-vis spectra of NTS-0H-xh and NTS-61H-xh.	6
Fig. S10 XRD patterns of CTS-yd and NTS-yd.	6
Fig. S11 Relative crystallinity curves of CTS-yd and NTS-yd.	7
Fig. S12 UV-vis spectra of CTS-yd and NTS-yd.	7
Table S1 Textural properties of CTS-1 and synthesized TS-1 samples.	8
Table S2 Comparison of titanium-rich TS-1 synthesized by hydrothermal methods.	9
References	10

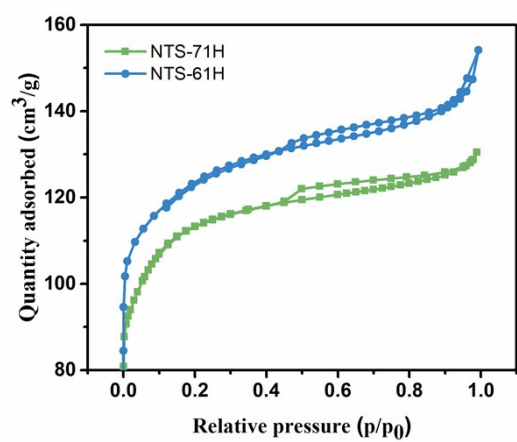


Fig. S1 N₂ adsorption–desorption isotherms of NTS-61H and NTS-73H.

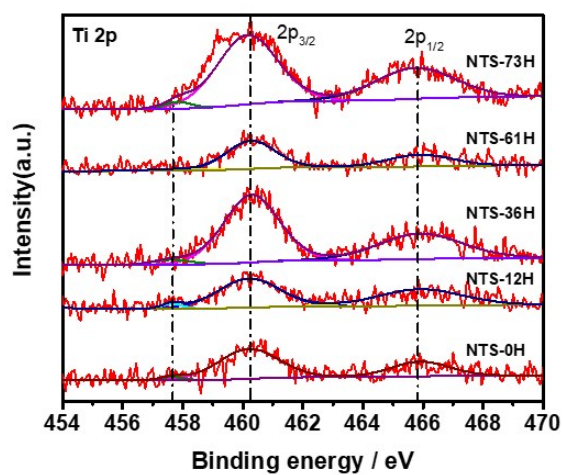


Fig. S2 The XPS spectra of Ti 2p of NTS-0H, NTS-12H, NTS-36H, NTS-61H and NTS-73H.

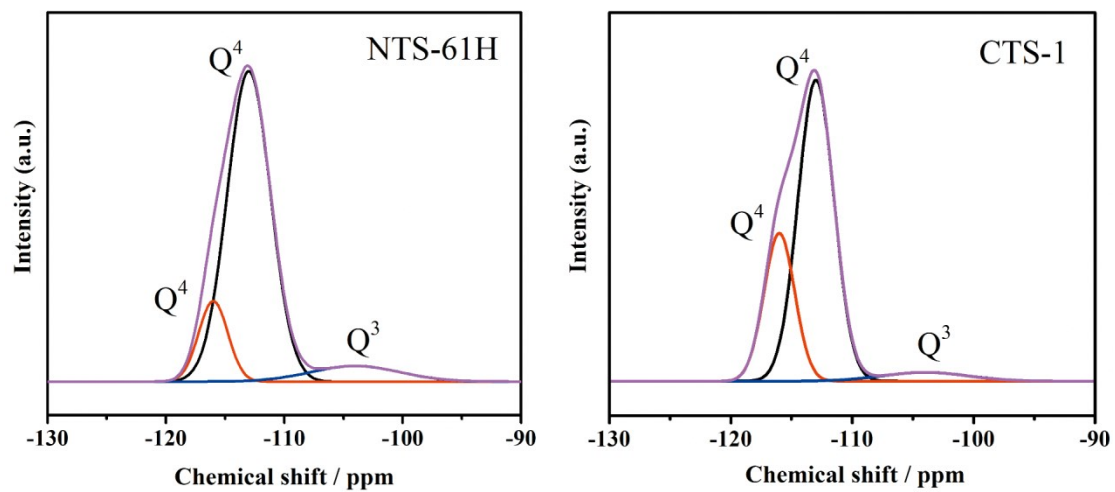


Fig. S3 ^{29}Si MAS NMR spectra of NTS-61H and CTS-1.

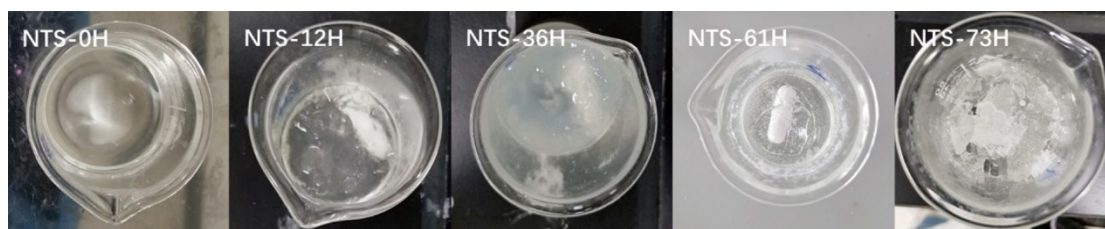


Fig. S4 Photos of initial synthetic mixtures with different amount of H_3BTC .

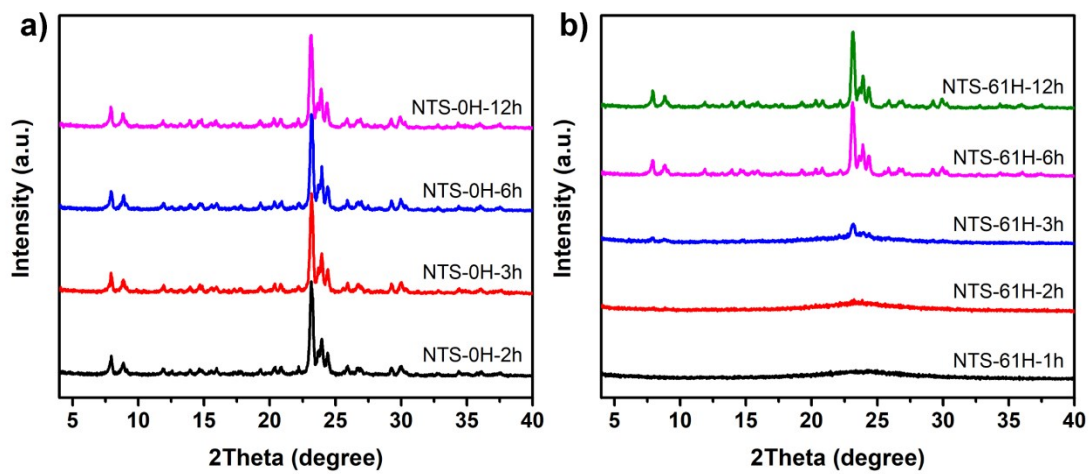


Fig. S5 XRD patterns of a) NTS-0H-xh samples and b) NTS-61H-xh samples.

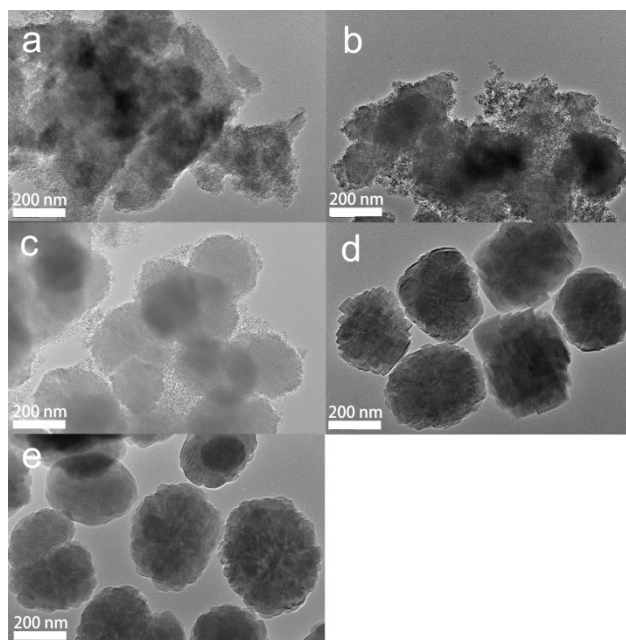


Fig. S6 TEM images of a) NTS-61H-1h, b) NTS-61H-2h, c) NTS-61H-3h, d) NTS-61H-6h, e) NTS-61H-12h.

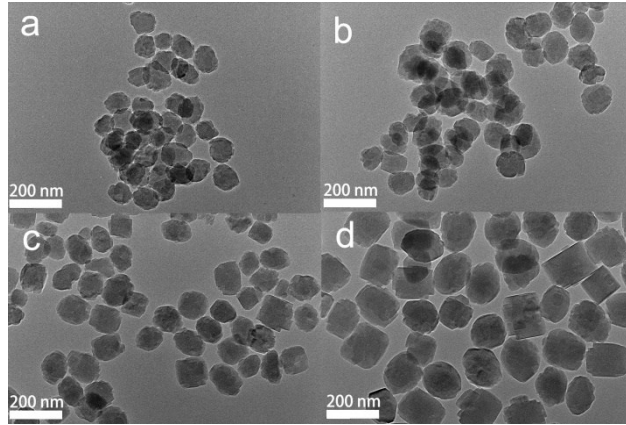


Fig. S7 TEM images of a) NTS-0H-2h, b) NTS-0H-3h, c) NTS-0H-6h, d) NTS-0H-12h.

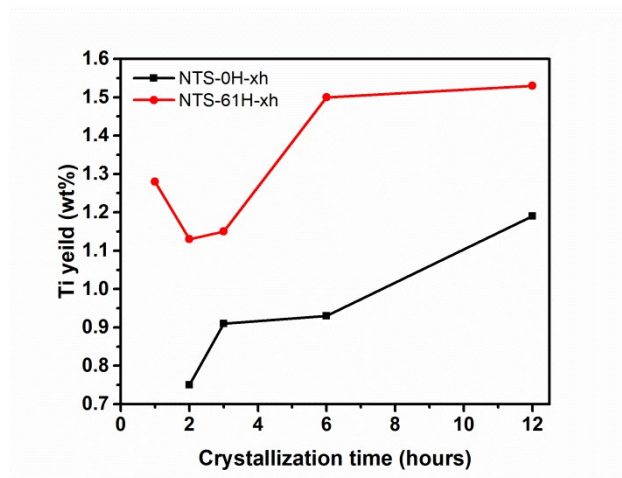


Fig. S8 Respective yields of Ti in NTS-0H-xh and NTS-61H-xh.

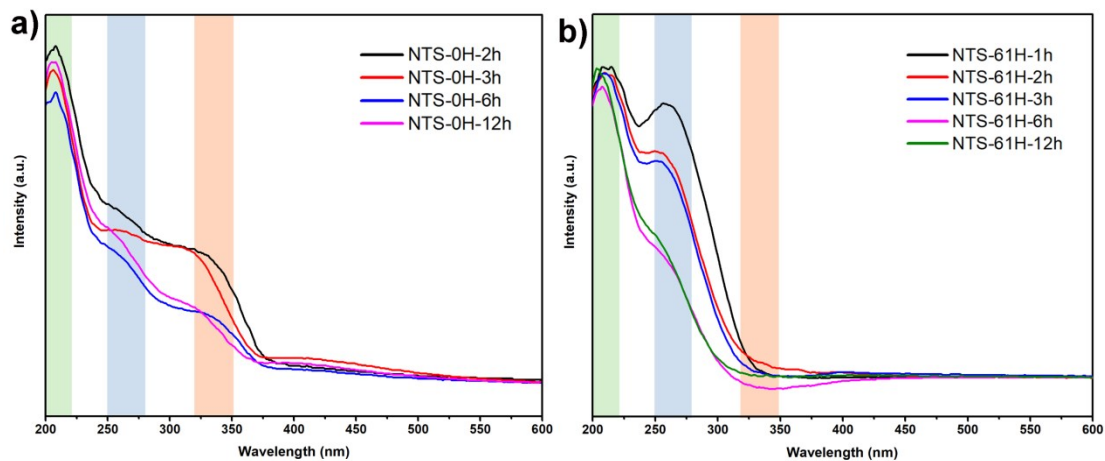


Fig. S9 UV-vis spectra of a) NTS-0H-xh and b) NTS-61H-xh.

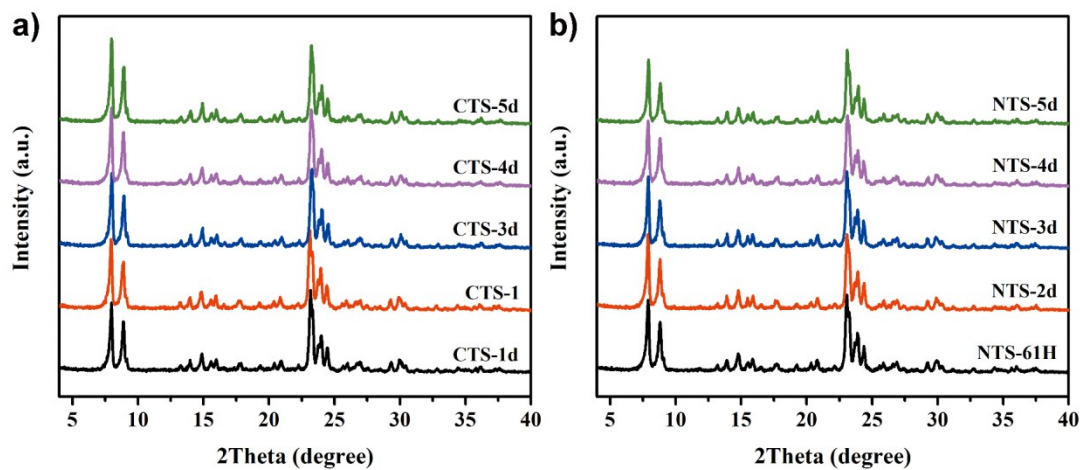


Fig. S10 XRD patterns of a) CTS-yd samples and b) NTS-yd samples.

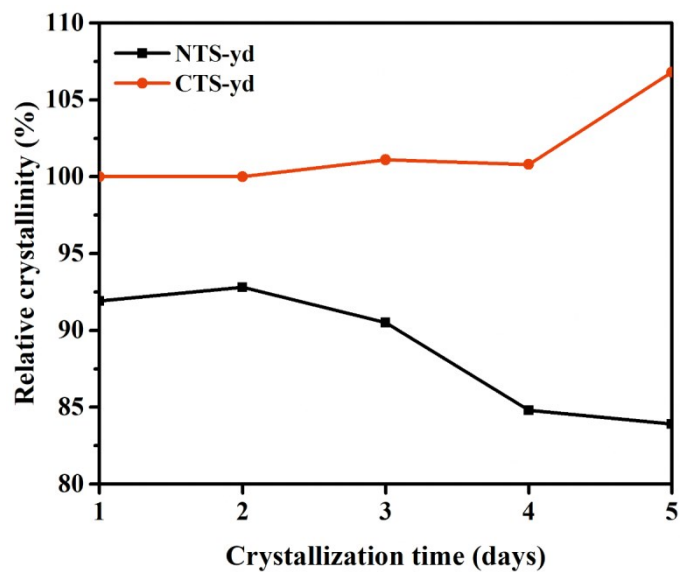


Fig. S11 Relative crystallinity curves of CTS-yd samples and NTS-yd samples (the crystallinity of CTS-1 as the standard 100%).

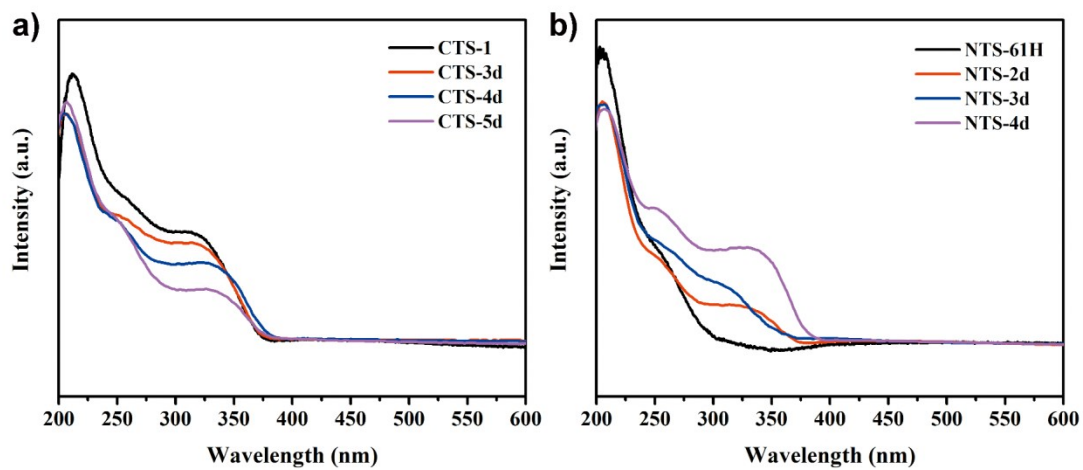


Fig. S12 UV-vis spectra of CTS-yd samples and NTS-yd samples.

Table S1 Textural properties of CTS-1 and synthesized TS-1 samples.

	S_{BET}	S_{micro}	S_{ext}	V_{total}	V_{micro}	V_{meso}
	$(\text{m}^2 \text{g}^{-1})^{\text{a}}$	$(\text{m}^2 \text{g}^{-1})^{\text{b}}$	$(\text{m}^2 \text{g}^{-1})^{\text{b}}$	$(\text{cm}^3 \text{g}^{-1})^{\text{c}}$	$(\text{cm}^3 \text{g}^{-1})^{\text{d}}$	$(\text{cm}^3 \text{g}^{-1})^{\text{e}}$
CTS-1	385	278	108	0.24	0.13	0.11
NTS-0H	397	264	133	0.28	0.12	0.16
NTS-12H	391	221	169	0.46	0.12	0.34
NTS-36H	393	224	169	0.39	0.12	0.27
NTS-61H	358	230	128	0.24	0.13	0.11
NTS-73H	344	218	126	0.20	0.12	0.08

^a Surface area was calculated from the nitrogen adsorption isotherm using the BET method.

^b S_{micro} (micropore area), S_{ext} (external surface area) were calculated using the t-plot method.

^c V_{total} (total pore volume) at $P/P_0 = 0.99$.

^d V_{micro} (micropore volume) was calculated using the t-plot method.

^e V_{meso} (mesopore volume) = V_{total} (total pore volume) - V_{micro} .

Table S2 Comparison of titanium-rich TS-1 synthesized by the hydrothermal methods.

Crystallization modifier	Synthetic method	Si/Ti	Ti wt%	Time-gel. (hours) ^d	Crystallization temperature (°C)	Time-cry. (days) ^e	Ref.
H ₃ BTC	Hydrothermal method	48.5 ^a		4.5	180	1	This work
(NH ₄) ₂ CO ₃	Hydrothermal method	65-66 ^b		>2.5	160	3	1
(NH ₄) ₂ CO ₃	Hydrothermal method and post-treatments	34 ^a			170	6	2
(NH ₄) ₂ CO ₃	Hydrothermal method and post-treatments	43.1 ^a		>4.5	170	6	3
PAA	Hydrothermal method	44 ^a		>0.5	170	7	4
IPA	Hydrothermal method		3.08-9.92 ^c	>8.5	170	7	5
Triton X-100	Rotation hydrothermal method	33.9 ^a		>8	170	4	6

^a The elemental compositions in the bulk were determined by ICP; ^b Molar ratio of Si to Ti was determined by energy dispersive X-ray spectroscopy (EDS); ^c The percentage content of titanium in the catalysts was determined by XRF method; ^d Time of gel preparation; ^e Time of hydrothermal crystallization.

References

1. M. Shakeri and S. B. Dehghanpour, Rational synthesis of TS-1 zeolite to direct both particle size and framework Ti in favor of enhanced catalytic performance, *Microporous Mesoporous Mater.*, 2020, **298**, 110066.
2. W. Fan, R.-G. Duan, T. Yokoi, P. Wu, Y. Kubota and T. Tatsumi, Synthesis, crystallization mechanism, and catalytic properties of titanium-rich TS-1 free of extraframework titanium species, *J. Am. Chem. Soc.*, 2008, **130**, 10150-10164.
3. W. Jiao, Y. He, J. Li, J. Wang, T. Tatsumi and W. Fan, Ti-rich TS-1: A highly active catalyst for epoxidation of methallyl chloride to 2-methyl epichlorohydrin, *Appl. Catal., A*, 2015, **491**, 78-85.
4. J. Wang, Y. Zhao, T. Yokoi, J. N. Kondo and T. Tatsumi, High-Performance Titanosilicate Catalyst Obtained through Combination of Liquid-Phase and Solid-Phase Transformation Mechanisms, *Chemcatchem*, 2014, **6**, 2719-2726.
5. A. Wroblewska, J. Tolpa, D. Klosin, P. Miadlicki, Z. C. Koren and B. Michalkiewicz, The application of TS-1 materials with different titanium contents as catalysts for the autoxidation of alpha-pinene, *Microporous Mesoporous Mater.*, 2020, **305**, 110384.
6. T. Zhang, X. Chen, G. Chen, M. Chen, R. Bai, M. Jia and J. Yu, Synthesis of anatase-free nano-sized hierarchical TS-1 zeolites and their excellent catalytic performance in alkene epoxidation, *J. Mater. Chem. A*, 2018, **6**, 9473-9479.